64. Meeks, M. L. *et al. Science* **165,** 180 (1969).
65. Turner, B. E. *et al. Astrophys. J. Lett.* **198,** L125 (1975).
66. Phillips, T. G. *et al. Astrophys. J. Lett.* **22,** L59 (1978).
67. Tucker, K. D. *et al. Astrophys. J. Lett.* **193,** L115 (1974).
68. Snyder, L. E. & Buhl, D. *Astrophys. J. Lett.* **163,** L47, (1971).
69. Gottlieb, C. A. *et al. Astrophys. J.* **202,** 655 (1975).
70. Jefferts, K. B. *et al. Astrophys. J. Lett.* **179,** L57 (1973).
71. Penzias, A. A. *et al. Astrophys. J.* **211,** 108 (1977).
72. Wilson, R. W. *Astrophys. J. Lett.* **186,** L77 (1972).
73. Linke, R. A. *et al. Astrophys. J.* **214,** 50 (1977).
74. Kaifu, N. *et al. Astrophys. J. Lett.* **191,** L135 (1974).
75. Snyder, L. E. & Buhl, D. *Bull. Am. astr. Soc.* **3,** 388 (1971).
76. Saykally, R. J. *et al. Astrophys. J. Lett.* **204,** L143 (1976).
77. Snell, R. L. & Wooten, H. A. *Astrophys. J. Lett.* **216,** L111 (1977).
78. Godfrey, P. D. *et al. Mon. Not. R. astr. Soc.* **180,** 83P (1977).
79. Brown, R. D. *et al. Nature* **262,** 672 (1976).
80. Brown, R. D. *et al. Mon. Not. R. astr. Soc.* **180,** 87P (1977).
81. Buhl, D. & Snyder, L. E. *Nature* **228,** 267 (1970).
82. Klemperer, W. *Nature* **227,** 1230 (1970).
83. Woods, R. G. *Phys. Rev. Lett.* **35,** 1269 (1975).
84. Hollis, J. M. *et al. Astrophys. J.* **200,** 584 (1975).
85. Snyder, L. E. *et al. Astrophys. J.* **209,** 67 (1976).
86. Hollis, J. M. *et al. Astrophys. J. Lett.* **209,** L83 (1976).
87. Guélin, M. *et al. Astrophys. J. Lett.* **217,** L165 (1977).
88. Jennings, D. E. & Fox, K. *Astrophys. J.* **227,** 433 (1979).
89. Langer, W. D. *et al. Astrophys. J. Lett.* **225,** L139 (1978).
90. Guelin, M. & Thaddeus, P. *Astrophys. J. Lett.* **227,** L139 (1979).
91. Snyder, L. E. *et al. Astrophys. J. Lett.* **208,** L91 (1976).
92. Turner, B. E. *Astrophys. J.* **193,** L83 (1974).
93. Green, S. *et al. Astrophys. J. Lett.* **193,** L89 (1974).
94. Saykally, R. J. *et al. Astrophys. J. Lett.* **205,** L101 (1976).
95. Snyder, L. E. *et al. Astrophys. J. Lett.* **218,** L61 (1977).
96. Thaddeus, P. & Kutner, M. L. *Astrophys. J. Lett.* **176,** L75 (1972).
97. Ulich, B. L., Hollis, J. M. & Snyder, L. E. *Astrophys. J. Lett.* **217,** L105 (1977).
98. Jefferts, K. B. *et al. Astrophys. J. Lett.* **168,** L111 (1971).
99. Solomon, P. M. *et al. Astrophys. J.* **185,** L63 (1973).
100. Hollis, J. M. & Ulich, B. L. *Astrophys. J.* **214,** 699 (1977).
101. Snyder, L. E. *et al. Astrophys. J. Lett.* **198,** L81 (1975).
102. Cheung, A. C. *et al. Phys. Rev. Lett.* **21,** 1701 (1968).
103. Turner, B. E. *et al. Astrophys. J. Lett.* **219,** L43 (1978).
104. Kuiper, E. N. R. *et al. Astrophys. J. Lett.* **219,** L49 (1978).
105. Wilson, T. L. & Pauls, T. *Astr. Astrophys.* **73,** L10 (1979).
106. Morris, M. *et al. Astrophys. J.* **186,** 501 (1973).
107. Ridgeway, *et al. Nature* **264,** 345 (1976).
108. Snyder, L. E. *et al. Phys. Rev. Lett.* **22,** 679 (1969).
109. Langer, W. D. *et al. Astrophys. J. Lett.* **232,** L169 (1979).
110. Zuckerman, B. *et al. Astrophys. J.* **160,** 485 (1970).
111. Zuckerman, B. *et al. Astrophys. J. Lett.* **157,** L167 (1969).
112. Whiteoak, J. B. & Gardner, F. F. *Astrophys. Lett.* **11,** 15 (1977).
113. Gardner, F. F. *et al. Astrophys. Lett.* **9,** 181 (1971).
114. Tucker, K. D. *et al. Astrophys. J. Lett.* **227,** L143 (1979).
115. Buhl, D., Snyder, L. E. & Edrich, J. *Astrophys. J.* **177,** 625 (1972).
116. Snyder, L. E. & Buhl, D. *Astrophys. J.* **177,** 619 (1972).
117. Sinclair, M. W. *et al. Aust. J. Phys.* **26,** 85 (1973).
118. Doherty, L. H., MacLeod, J. M. & Oka, T. *Astrophys. J. Lett.* **192,** L157 (1974).
119. Guélin, M. & Thaddeus, P. *Astrophys. J. Lett.* **212,** L81 (1977).
120. Green, S. *Astrophys. J. Lett.* **212,** L87 (1977).
121. Linke, R. A. *et al. Astrophys. J. Lett.* **234,** L139 (1979).
122. Fox, A. K. & Jennings, D. E. *Astrophys. J. Lett.* **226,** L43 (1978).
123. Godfrey, P. D. *et al. Astrophys. Lett.* **13,** 119 (1973).
124. Turner, B. E. *Astrophys. J. Lett.* **213,** L75 (1977).
125. Turner, B. E. *et al. Astrophys. J. Lett.* **201,** L149 (1975).
126. Zuckerman, B. *et al. Astrophys. J. Lett.* **163,** L41 (1971).
127. Winnewisser, G. & Churchwell, E. *Astrophys. J. Lett.* **200,** L33 (1975).
128. Guélin, M. Green, S. & Thaddeus, P. *Astrophys. J. Lett.* **224,** L27 (1978).
129. Turner, B. E. *Astrophys. J. Lett.* **163,** L35 (1971).
130. Morris, M. *et al. IAU Symp.* No. 52 (1973).
131. Morris, M. *et al. Astrophys. J.* **205,** 82 (1976).
132. Churchwell, E., Walmsley, C. M. & Winnewisser, G. *Astr. Astrophys.* **54,** 925 (1977).
133. Wannier, P. G. & Linke, R. A. *Astrophys. J.* **226,** 817 (1978).
134. Gardner, F. F. & Winnewisser, G. *Astrophys. J. Lett.* **197,** L73 (1975).
135. Ball, J. A. *Astrophys. J. Lett.* **162,** L203 (1970).
136. Gottlieb, C. A. *et al. Astrophys. J.* **227,** 422 (1979).
137. Solomon, P. M. *et al. Astrophys. J. Lett.* **168,** L107 (1971).
138. Lovas, F. J. *et al. Astrophys. J.* **209,** 770 (1976).
139. Rubin, R. H. *et al. Astrophys. J. Lett.* **169,** L39 (1971).
140. Gottlieb, C. A. *et al. Astrophys. J.* **182,** 699 (1973).
141. Kaifu, N. *et al. Astrophys. J. Lett.* **191,** L135 (1974).
142. Fourikis, N. *et al. Astrophys. J. Lett.* **191,** L139 (1974).
143. Fourikis, N. *et al. Astrophys. J. Lett.* **212,** L33 (1977).
144. MacLeod, J. M. *et al. Astrophys. J.* **231,** 401 (1979).
145. Snyder, L. E. & Buhl, D. *Nature, phys. Sci.* **243,** 45 (1973).
146. Gottlieb, C. A. *Molecules in Galatic Environment* (eds Gordon, M. A. & Snyder, L. E.) (Wiley, New York, 1973).
147. Fourikis, N. *et al. Aust. J. Phys.* **27,** 425 (1974).
148. Gardner, F. F. & Winnewisser, G. *Astrophys. J. Lett.* **195,** L127 (1975).
149. Johnson, D. R. *et al. Astrophys. J.* **218,** 370 (1977).
150. Gardner, F. F. & Winnewisser, G. *Mon. Not. R. astr. Soc.* **185,** 57P (1978).
151. Avery, L. W. *et al. Astrophys. J. Lett.* **205,** L173 (1976).
152. Broten, N. W. *et al. Astrophys. J. Lett.* **209,** L143 (1976).
153. Walmsley, C. M. *et al.* preprint (1979).
154. Brown, R. D. *et al. Astrophys. J. Lett.* **197,** L29 (1975).
155. Zuckerman, B. *et al. Astrophys. J. Lett.* **196,** L99 (1975).
156. Snyder, L. E. *et al. Astrophys. J. Lett.* **191,** L79 (1974).
157. Johnson, D. R. *et al. Astrophys. J.* **218,** 370 (1977).
158. Kroto, H. W. *et al. Astrophys. J. Lett.* **219,** L133 (1978).
159. Little, L. T. *et al. Mon. Not. R. astr. Soc.* **183,** 45P (1978).
160. Broten, N. W. *et al. Astrophys. J. Lett.* **223,** L105 (1978).
161. Knowles, S. H. *Science* **163,** 1055 (1969); **166,** 221 (1969).
162. Rydbeck, O. E. H. *et al. Nature* **246,** 466 (1973).
163. Frerking, M. A. *et al. Astrophys. J. Lett.* **234,** L143 (1979).

ARTICLES

Interstellar extinction in the Large Magellanic Cloud

K. Nandy*, D. H. Morgan*, A. J. Willis†, R. Wilson†, P. M. Gondhalekar‡ & L. Houziaux§

* Royal Observatory, Blackford Hill, Edinburgh EH9 3HJ, UK; † Department of Physics and Astronomy, University College, London, Gower Street, London WC1E 6BT, UK; ‡ SRC Appleton Laboratory, Ditton Park, Slough, Buckinghamshire, UK; § Institut d'Astrophysique, Université de Liège, Belgium

Recent UV observations together with complementary visible data of several reddened and comparison stars of similar spectral types in the Large Magellanic Cloud have been used to study the interstellar extinction in that galaxy. Most of the reddened stars studied here are located within 2° of 30 Doradus and show remarkably high extinction in the far UV, suggesting a large abundance of small particles. From the optical wavelength to 2,600 Å *the normalised extinction curves of the LMC stars are similar to the mean galactic extinction law.*

THE Large Magellanic Cloud (LMC) is the nearest extragalactic system and a preliminary study of the UV spectra of LMC members shows the importance of the IUE[1] for stellar and interstellar work in the Magellanic Clouds. The Clouds contain dust though to a lesser extent than the Galaxy. A recent survey of the chemical composition of H II regions in the Magellanic Clouds[2] reveals that oxygen is deficient in these galaxies by about a factor of four relative to the Orion nebula. The composition of the interstellar dust and gas in the Clouds provides important information on the origin of the dust and the chemical enrichment of the interstellar media in these galaxies.

The wavelength dependence of interstellar extinction over a wide range of wavelengths from the visible to the UV depends on the composition and relative abundances of the agents responsible for scattering and absorption[3]. The characteristic feature of the galactic extinction curve is the broad symmetric absorption band ($\Delta\lambda \sim 750$ Å) centred near 2,200 Å (ref. 4). Earlier attempts to determine the UV extinction law in the LMC, using surface brightness measurements obtained with the

0028–0836/80/080725—05$01.00

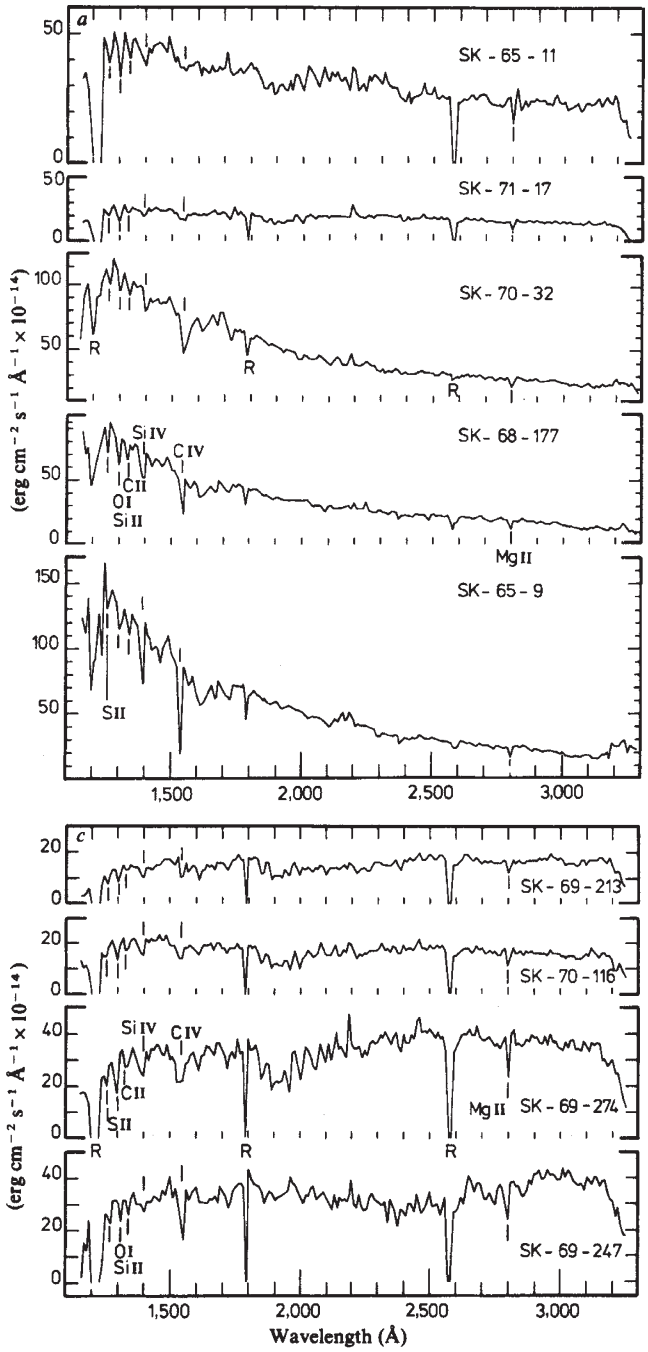

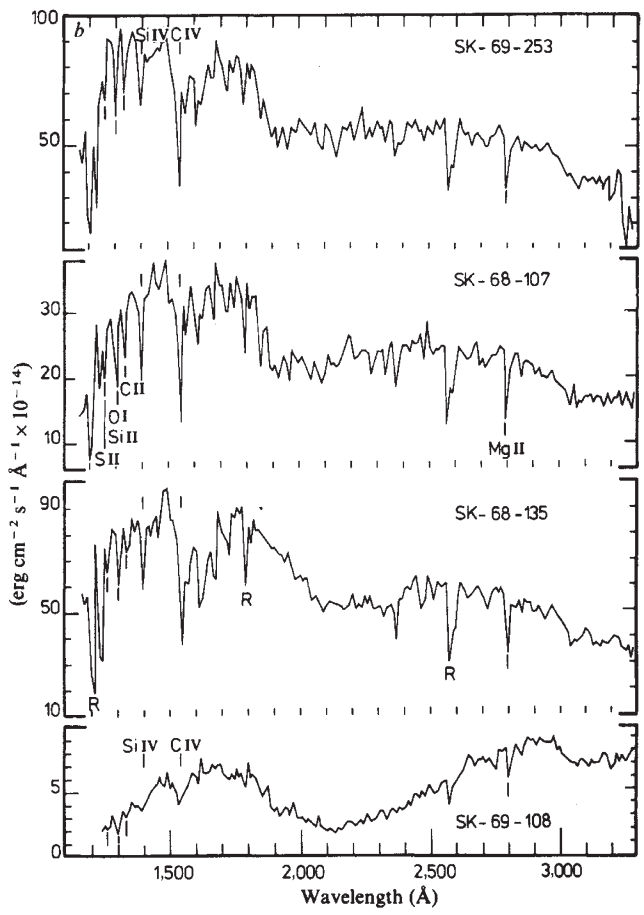

Fig. 1 *a*, The IUE spectra of five comparison LMC stars showing the major interstellar lines (S II, O I, Si II, C II, Mg II), stellar C IV and Si IV lines, and the fiducial marks indicated by R. *b*, *c*, The IUE spectra of eight reddened LMC stars. The lines shown are as *a*.

S2/68 (ref. 5) and ANS experiments[6,7] have led to discrepant results. The detection of the 2,200 Å feature in the spectrum of a reddened LMC member, SK-69-108, has recently been reported[8]. This article presents further observations, in both the visible and the UV, of a larger sample of LMC stars to study interstellar extinction in the LMC.

Observations

The IUE[9,10] controlled from the ESA satellite tracking station at Villafranca, Spain, was used in its low resolution mode ($\Delta\lambda \sim 6$ Å) to obtain UV spectra of the reddened and comparison stars. Complementary visible spectra which extend from 3,980 to 6,140 Å were obtained at a dispersion of 110 Å mm^{-1} using the image dissector scanner at the Cassegrain focus of the 3.6 m telescope of the ESO at La Silla, Chile. Table 1 lists the reddened and comparison stars observed, together with their coordinates, photometric data and spectral types[11–13].

The reduced UV spectra provided before August 1979 by the IUE ESA Observatory contained ITF errors in the short wavelength channel. Consequently, the photometric correction of the raw images of these spectra was repeated with the correct intensity transfer functions (ITF) using a program developed by J. Fettle (personal communication), and the corrected spectra extracted. The UV spectra in the long wavelength channel were provided by the ESA Observatory. Absolute fluxes were obtained using the adopted sensitivity calibration curve[14].

The wavelength scales were checked by examining the positions of the principal interstellar lines: 1,260 Å (blend of Si II and S II), 1,303 Å (O I, Si II), 1,335 Å (C II), 2,342 Å (Fe II), 2,382 Å (Fe II), 2,598 Å (Fe II) and 2,798 Å (Mg II). The wavelength scales of the reduced spectra were found in all cases to be accurate to ±4 Å. The raw images were checked for fiducial marks, noise, spikes and saturation effects. Data affected by saturation and fiducial marks were excluded. Except for the short wavelength spectrum of SK-69-213, all spectra were well exposed with average signal over all spectral ranges of interest lying over 100 DN (IUE data number). The UV flux distributions in absolute units smoothed over 10 Å bands of the comparison and reddened stars are shown in Fig. 1*a*–*c*.

The visible spectra were obtained on one night (25 December 1978). The wavelength and flat field calibration of the data, recorded on magnetic tape, was performed at ESO, Geneva, using He–Ar and flat field spectra taken immediately before the stellar observations. As the difference between the air masses at the beginning and the end of the observing night was small, the visible spectra were corrected for atmospheric extinction using the mean law appropriate for La Silla (by Dr H. Pederson of the ESO). The visible spectra were reduced to give data points every 1.5 Å and in the subsequent analysis average counts in 60 Å wavelength intervals from $\lambda^{-1} = 1.66$ to 2.54 μm^{-1} were utilised. The photometric accuracy of the average counts is ~±3%.

Measurement of interstellar extinction

The analysis of the spectral features in the UV and visible data obtained will be given elsewhere. Note, however, that the reddened stars listed in Table 1 clearly show the diffuse interstellar feature at 4,430 Å similar to that observed in reddened stars in the galaxy. The equivalent width of this feature is compatible with that computed from the colour-excess, $E(B-V)$, from the mean galactic relationship between W_{4430} and $E(B-V)$ (ref. 15).

To measure the extinction in the visible wavelength range, a set of extinction curves was derived for each of the reddened stars using comparison stars, and a mean extinction curve was determined for each reddened star, thus reducing the errors introduced by possible spectral type mismatch. The extinction in magnitudes, $\Delta m(\lambda)$ has been normalised to $\Delta m = 0$ at 5,500 Å (the effective wavelength of the V-band) and $\Delta m = 1$ at 4,300 Å (the effective wavelength of the B-band). Within observational errors, the individual extinction curves in the visible agree well thereby allowing a mean extinction curve to be constructed. The mean curve was computed in the wavelength range, $\lambda^{-1} = 1.66$–2.94 μm^{-1} with r.m.s. error $<\pm 0.3$ mag, and extended to the U-band using the available UBV photometric data. This mean curve seems to be identical to the mean galactic extinction law in the visible as derived by Seaton[16].

For the measurement of interstellar extinction in the UV, the comparison stars SK-67-108 and SK-67-111, which were observed with the small (3×3 arc s) IUE spectrograph slits, were excluded. To improve the photometric accuracy of the UV data, the stellar fluxes were averaged in 50 Å bands from 1,150 to 3,000 Å. The mean photometric accuracy of a single observation has been estimated from the difference in the colours $(m_\lambda - m_{2,900Å})$ of stars with more than one observation: it is ~±0.05 mag except near the extremities of the wavelength channels where it is much larger, about ±0.3 mag.

The UV extinction has been measured for pairs of reddened and comparison stars which match in spectral type. The extinction, Δm is normalised to $\Delta V = 0$ and $\Delta E(B-V) = 1$, where ΔV is the difference in the V magnitudes and $\Delta E(B-V)$ is the difference in the colour-excesses of the reddened and comparison stars. The UV extinction curves for eight reddened stars are shown in Fig. 2; the ordinate is the normalised extinction,

$$\Delta m = \frac{A_\lambda - A_V}{E(B-V)}$$

Discussion

Apart from photometric errors, the major source of error in the extinction measurements constructed from the pairs of reddened and comparison stars is the mismatch in spectral type and luminosity class. For the sample of LMC stars studied here, the spectral type error is estimated to be ~±1 subclass. This estimate is based on an examination of the important spectral features both in the visible and in the UV. However, the difference in absolute magnitude, ΔM_V between the reddened and comparison stars is ~−1.6 mag. Galactic supergiants have a flux deficiency in the far UV (shortward of 1,600 Å) as compared with giants and dwarfs[17]. However, from a study of the spectra of galactic stars which appear in the Ultraviolet Bright-Star Catalogue[18] it is found that the UV flux distributions of B0-B3Ia stars do not differ significantly from those of B0-B3Ib stars, the differences being well within the photometric errors. The error in the measured extinction due to spectral type mismatch of ±1 subclasses per unit normalising factor is ~±0.2 mag near 2,740 Å increasing to ~±0.4 mag at 1,400 Å.

The interesting feature of Fig. 2 is that shortward of $\lambda^{-1} = 3.8$ μm^{-1} the extinction curve for SK-69-108 is clearly different from those of the other stars: shortward of 5.5 μm^{-1} the extinction for SK-69-108 is on average 2 mag lower than that for the other stars and near 2,200 Å (4.6 μm^{-1}) it is ~1 mag greater. But longward of 2,600 Å ($\lambda^{-1} = 3.8$ μm^{-1}), the normalised extinction values for all the stars are the same. Note that the reddened star SK-69-108 is situated in the bar, while the other reddened stars are located to the north-east of the bar within 2° of the 30 Doradus region, a site of recent star formation. This raises the interesting possibility that the extinction properties of the dust in the latter region may differ from those of the dust in

Table 1 Programme stars observed in the LMC

Star	RA (1975)	Dec (1975)	Spectral type	V	$B-V$	$U-B$	Spectral range observed
Reddened stars							
SK-68-107	5h 30.8 min	−68° 26′	B0Ia	12.22	0.03	−0.82	Visible to UV
SK-68-135	5 38.0	−68 56	09.5I	11.36	0.00	−0.86	Visible to UV
SK-69-108	5 20.1	−69 54	B3I	12.10	0.27	−0.49	Visible to UV
SK-69-213	5 36.4	−69 12	B1	11.97	0.10	−0.75	UV
SK-69-253	5 39.7	−69 28	B0I	11.23	−0.02	−0.81	Visible to UV
SK-69-247	5 39.1	−69 31	B6I	10.42	0.17	−0.54	UV
SK-69-274	5 41.7	−69 49	B2.5Ia	11.21	0.04	−0.74	UV
SK-70-116	5 49.3	−70 3	B2Ia	12.05	0.11	−0.72	UV
Comparison stars							
SK-65-9	4 59.2	−65 51	B1	12.72	−0.22	−1.07	UV
SK-65-11	4 59.3	−65 45	B5I	11.66	−0.04	−0.69	UV
SK-67-108*	5 26.5	−67 38	B0	12.56	−0.20	−1.05	Visible to UV
SK-67-110	5 26.9	−67 29	B1:	11.62	−0.07	−0.94	Visible
SK-67-111*	5 26.9	−67 30	0B	12.57	−0.20	−1.03	Visible to UV
SK-68-177	5 53.0	−68 14	B2	12.93	−0.18	−0.96	UV
SK-70-32	5 0.5	−70 13	B0I	13.10	−0.21	−1.01	UV
SK-71-17	5 22.0	−71 58	B3Ia (ref. 13)	12.29	−0.06		UV
SK-69-249	5 39.2	−69 30	B0.5	(10.6)			Visible

* IUE observations recorded using the small spectrograph aperture. All other IUE data were obtained using the large aperture. Figure in brackets is photographic V-mag (ref. 11).

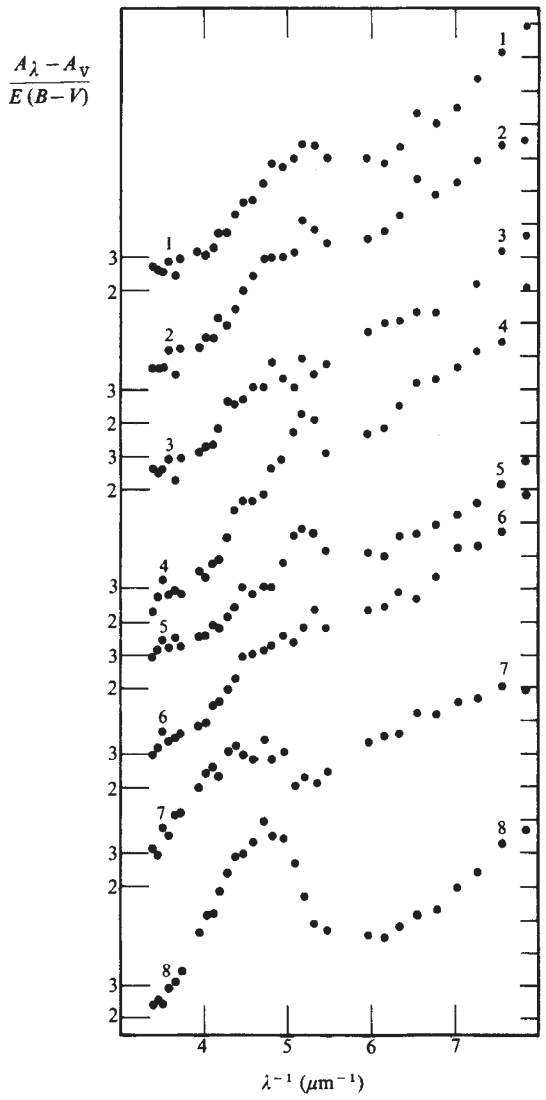

Fig. 2 Individual extinction curves normalised to $V=0$ and $E(B-V)=1$ derived from IUE observations. The numbers 1–8 denote the following pairs of reddened and comparison stars: 1, SK-68-107, SK-70-32; 2, SK-69-253, SK-70-32; 3, SK-68-135, SK-70-32; 4, SK-69-274, SK-68-177 and SK-71-17; 5, SK-70-116, SK-68-177; 6, SK-69-213, SK-65-9; 7, SK-69-274, SK-65-11; 8, SK-69-108, SK-71-17.

the bar. As the extinction curves of seven of the stars have similar shapes, they have been combined to give a mean curve. This curve is shown in Fig. 3 with the extinction curve for SK-69-108; also shown in Fig. 3 are the mean visible extinction curve as determined for the LMC stars, and for comparison the galactic extinction law of Seaton[16]. The mean normalising factor being 4, the r.m.s. error bar shown in the mean extinction curve can be explained in terms of the observational errors. Within this error, the extinction curve for SK-69-108 is close to the galactic law, while the mean extinction curve for other stars shows an increase in extinction by ~3 mag in the far UV shortward of $\lambda^{-1} = 6\ \mu m^{-1}$, which is much larger than twice the r.m.s. error.

The 2,200 Å feature for the mean curve seems to be weaker than that for the galactic law, but not as much as suggested by Koornneef[7]. For example, the colour-excess ratio $E(2{,}200-2{,}500)/E(B-V)$ has a mean value of 2 for the seven stars, (2.7 for SK-69-108) and 2.5 for galactic stars. Between 4.6 and 5.5 μm^{-1} the mean extinction curve does not decrease as much as it does in the case of SK-69-108 and in the galactic law. This is partly due to the broad 1,920 Å feature ($\Delta\lambda \sim 100$ Å) of stellar origin, being much stronger in the spectra of five of the seven reddened stars than in the comparison stars. This 1,920 Å feature is due to a blend of Fe III lines, first detected in the S2/68 spectra of luminous stars and found to be independent of spectral type[19]. The structure near $\lambda^{-1} = 5.2\ \mu m^{-1}$ in the mean extinction curve is due to this stellar feature. But when corrected by using interpolated continua for the 1,920 Å feature, the extinction near 1,920 Å decreased by only a few tenths of a magnitude. Therefore the difference between the mean extinction curve for the seven stars and the galactic law as well as SK-69-108 seems to be real shortward of 2,200 Å. A possible explanation for the increasing extinction in the far UV for the LMC region around 30 Doradus is that the relative abundance of small (a few hundred ångströms sized) dielectric particles is significantly greater than that in the interstellar medium in the solar neighbourhood.

The difference between the extinction curves for SK-69-108, located in the bar, and the other seven stars may indicate a regional difference in the extinction law in the LMC. Clearly further observations of reddened stars in the LMC bar are needed.

Conclusion

From the study of seven reddened stars located within 2° of 30 Doradus in a region to the north-east of the bar of the LMC, and five comparison stars, the mean extinction curve for this region shortward of 1,600 Å, shows significantly greater extinction than the mean galactic extinction law. This may be due to a relatively higher abundance of small (few hundred ångströms sized) dielectric particles. However, an eighth reddened star, SK-69-108, shows an UV extinction curve similar to the mean galactic law: but this star is located in the bar of the LMC, suggesting a possible regional variation of the far UV extinction law throughout the LMC.

The interstellar extinction curves of all the stars in the visible and near UV wavelength ranges show no significant differences from the mean galactic extinction law.

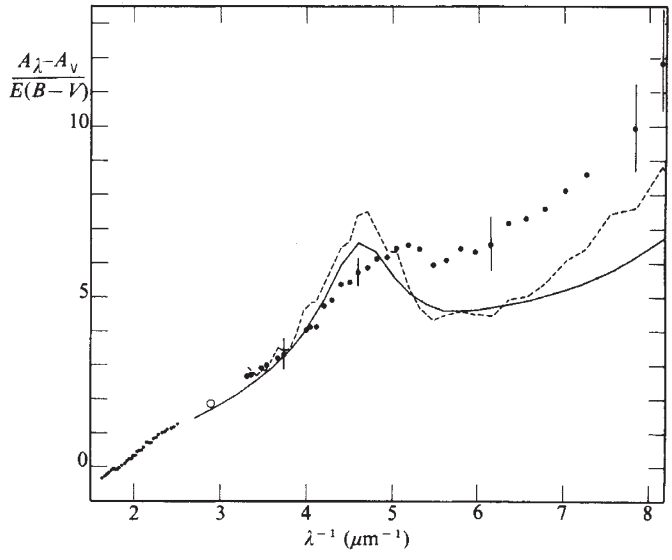

Fig. 3 The mean extinction curve derived from IDS data (dotted line); the mean extinction in the *U*-band (○); and the mean UV extinction curve for seven stars situated in a region within 2° of 30 Doradus (●). The dashed lines denote the extinction curve for SK-69-108 (situated in the bar). The solid line is the mean interstellar extinction law for the galaxy.

Received 13 August 1979; accepted 4 January 1980.

1. Nandy, K. & Morgan, D. H. *Mon. Not. R. astr. Soc.* (submitted).
2. Pagel, B. E., Edmunds, M. C., Fosbury, R. A. E. & Webster, B. L. *Mon. Not. R. astr. Soc.* **184**, 569 (1978).
3. Wickramasinghe, N. C. & Nandy, K. *Rep. Prog. Phys.* **35**, 157 (1972).
4. Nandy, K., Thompson, G. I., Wilson, R., Jamar, C. & Monfils, A. *Astr. Astrophys.* **44**, 63 (1975).
5. Nandy, K., Morgan, D. H. & Carnochan, D. J. *Mon. Not. R. astr. Soc.* **186**, 421 (1979).
6. Borgman, J. *Astr. Astrophys.* **69**, 245 (1978).
7. Koornneef, J. *Astr. Astrophys.* **67**, 179 (1978).
8. Nandy, K. & Morgan, D. H. *Nature* **276**, 478 (1978).
9. Boggess, A. *et al. Nature* **275**, 372 (1978).
10. Boggess, A. *et al. Nature* **275**, 377 (1978).
11. Sanduleak, N. (Cerro Tololo Inter-American Observatory Contr. No. 89, 1969).
12. Rousseau, J. *et al. Astr. Astrophys. Suppl.* **31**, 243 (1978).
13. Feast, M. W. *et al. Mon. Not. R. astr. Soc.* **121**, 337 (1960).
14. Bohlin, R. C., Holm, A. V., Savage, B. D. & Snijders, M. A. J. *Astr. Astrophys.* (in the press).
15. Hoŭziaux, L., Nandy, K. & Morgan, D. H. *Astr. Astrophys* (in the press).
16. Seaton, M. J. *Mon. Not. R. astr. Soc.* **187**, 73P (1979).
17. Thompson, G. I., Humphries, C. M. & Nandy, K. *Astrophys. J.* **187**, L81 (1974).
18. Jamar, C. *et al. ESA, Special Rep.* No. 27 (1976).
19. Nandy, K. *Highlts Astr.* **4**, 289 (1977).

An extensional origin for the Buchan and Witchground Graben in the North Sea

P. A. F. Christie

Department of Geodesy and Geophysics, Madingley Rise, Madingley Road, Cambridge CB3 0EZ, UK

J. G. Sclater

Department of Earth and Planetary Sciences, MIT, Cambridge, Massachusetts 02139

Seismic refraction and subsidence observations are used to explain the heatflow and subsidence properties of the North Sea.

THE theory of plate tectonics has been very successful in describing the creation of oceanic crust and accounting for the heat flow and subsidence anomalies observed over mid-ocean ridges[1]. However, the theory has not been able to explain the heat flow or subsidence of continental shelves or of epicontinental basins, in particular the Mesozoic and Cenozoic subsidence of the North Sea[2], which is considered here.

The main structural elements of the North Sea are the Viking and Central Graben, which underlie the axis of Tertiary sinking of the North Sea basin. These two major graben meet the Moray Firth Basin in the region of the Forties oil field, which also marks the confluence of the Buchan and Witchground Graben. The North Sea has been a centre of subsidence since the Devonian and although the graben system was initiated in Permo–Triassic times, most of the extension occurred from the Jurassic to Mid-Cretaceous[3]. Major rifting seems to have died out by the start of the Upper Cretaceous, giving way to a broad, general subsidence which allowed the accumulation of chalk, sands from the north-west and finally a thick sequence of Tertiary clays, shales and siltstones.

Although there are many models to account for the formation of shelves and inland basins (see refs 4–6), the most attractive are those based on the concepts used in describing the evolution of lithosphere as it moves away from the mid-ocean ridges[7–9]. In particular, on the basis of a high heat flow and a shallow Moho in the Aegean Sea, McKenzie[8,10] has suggested a simple stretching mechanism to account for the formation of sedimentary basins. In this model, thinning of the lithosphere occurs as a result of large scale extension whereby the surface area is increased by a factor b. If the extension is rapid and lithosphere is conserved, both the crust and the lithosphere decrease in thickness by a factor of $1/b$, causing a fault controlled isostatic subsidence of the surface and creating a thermal anomaly by the passive upwelling of hot asthenospheric material. As the thermal anomaly decays by conduction through the crust, the lithosphere thickens and subsides allowing, in the absence of further extension, the formation of a saucer shaped sedimentary basin. It can be shown[8] that the heat flow and subsidence history of a basin can be predicted as a function of the extension factor. If crustal material is conserved, a measurement of the depth to the Moho will indicate the amount of extension when compared with the Moho depth beneath a non-extended region. We show here that the decrease in Moho depth and increase in subsidence beneath the Witchground and Buchan Graben can be accounted for by a mechanism involving between 50 and 100% stretching of the lithosphere from the Jurassic through to the Mid-Cretaceous.

Seismic refraction data

The Marine Group at Cambridge University undertook the investigation of the velocity structure of the crust and upper mantle along a line parallel to and west of the main axis of Tertiary sinking in the North Sea (Fig. 1). The refraction experiment involved the shooting of three lines into sea bottom seismometers designed and built at Cambridge specifically for this experiment[11]. The main line, reversed over 400 km, was fired across the Witchground and Buchan Graben and was complemented by a shorter crustal control line at each end. Crustal and upper mantle phases were identified from the seismograms and interpretation of the travel time information was made using the method of time term analysis (see ref. 12). Using this approach, each shot and receiver location is assigned a delay time, or time term, which is due to the presence of the overburden between the shot or receiver point and the buried refractor. If the velocity structure in the overburden is known, then the delay time to the refractor beneath a particular site may be inverted to a depth value.

The analysis of the Firth of Forth profile revealed three refractors beneath the sediments with velocities of 5.7, 6.2 and 7.2 km s^{-1}. The Moho velocity is $\sim$8.16 km s^{-1}, a value taken from the Main Line as the Moho refraction was not reliably identified as a first arrival on this profile. The overall depth to the Moho is $\sim$30 km compared with 32–33 km observed for the Moho depth beneath the Southern Uplands as revealed by the LISPB experiment[13]. For the crustal control line at the north, a time term analysis of these arrivals, together with the crustal arrivals from Main Line shots, gave good control over the crustal refractors although the quality of the data was not as high as for the Firth of Forth Line. On the East Shetland Platform, the short range refractions gave a phase velocity of $\sim$4.1 km s^{-1}, which is consistent with Devonian Old Red Sandstone at shallow depth. This overlies an upper crustal layer of 5.7 km s^{-1}, which in turn covers a layer of 6.2 km s^{-1}. Both these values are in good

0028–0836/80/080729—04$01.00